New Tools for Terrain Gravimetry
NEWTON-g
Project number: 801221

Deliverable 3.3

On-field infrastructures

Lead beneficiary:	Istituto Nazionale di Geofisica e Vulcanologia (INGV)
Dissemination level:	Public
Version:	Final

NEWTON-g has received funding from the EC's Horizon 2020 programme, under the FETOPEN-2016/2017 call (Grant Agreement No 801221)

Document Information

Grant Agreement Number	801221
Acronym	NEWTON-g
Start date of the project	1 June 2018
Project duration (months)	48
Deliverable number	D3.3
Deliverable Title	On-field infrastructures
Due date of deliverable	31 May 2020
Actual submission date	06 June 2020
Lead Beneficiary	Istituto Nazionale di Geofisica e Vulcanologia (INGV)
Type	OTHER: Software, technical diagram, etc.
Dissemination level	PU - Public
Work Package	WP3 – Development of the gravity imager

Version	**Date**	**Author**	**Comments**
v.0	21/04/2020	A. Messina, D Contrafatto, D. Carbone, G. Siligato	Creation
v.1	01/06/2020	A. Messina, D Contrafatto	Revision
v.2	02/06/2020	E. de Zeeuw - van Dalfsen, M. Koymans	Revision
Final	06/06/2020	D, Carbone	Validation

TABLE OF CONTENTS

1. Introduction

The main objective of NEWTON-g is the development of a new measurement system for gravity observations, the gravity imager, that will permit to detect changes of the gravity field due to geophysical processes, with unparalleled spatio-temporal resolution. The gravity imager consists of an array of MEMS-based relative gravimeters, serving as “pixels”, anchored to an absolute quantum gravimeter.

During the last ~2 years of the project, the gravity imager will be field-tested at Mt. Etna volcano (Italy), where, due to persistent volcanic activity, measurable volcano-related gravity changes often develop, over different time and space scales. The volcano has also been well studied and is the site of a comprehensive existing monitoring network. Furthermore, its active crater zone can be reached by car. This combination of factors provides a unique and attractive natural laboratory for testing and benchmarking the new gravity instruments.

In the present document, we provide a detailed description of the field infrastructures that have been designed and developed to allow efficient functioning of the devices composing the gravity imager, during the deployment on the summit of Mt. Etna.

We also report on how the confinement measures put in place by the Italian government to fight the spread of the COVID-19 have delayed the development and installation of the field infrastructures, with respect to the plan agreed by the consortium during the “pre-deployment” meeting (5 – 7 February 2020).

This document is organized as follows:

section 2 provides information on the field infrastructures for the MEMS gravimeters;

section 3 describes the off-grid power system designed to permit continuous operation of the quantum gravimeter at the Pizzi Deneri Observatory (crater zone of Etna);

section 4 presents possible delay scenarios that could result from the COVID-19 pandemic.

2. Field infrastructures for the MEMS gravimeters

Harsh environmental conditions at the summit of Mt. Etna (snow and ice during winter, strong wind, lack of mains electricity, presence of corrosive gases) imply that special care must be taken in designing the field infrastructures aimed to (i) protect and power the gravity sensors and (ii) acquire, store and transmit the data to the main collector host.
Most MEMS devices composing the gravity imager will be installed at sites where no previous facility exists. Hence, a complete field infrastructure (MEMS station) has been designed, ensuring full protection and functionality of the MEMS gravimeters against severe field conditions (Fig. 1). Several considerations influenced the design of the MEMS station, including power supply sizing, optimal tilt angle of the solar panel at each site, suitable coupling between the gravimeter and the ground, etc. It has also been necessary to take into account the constraints imposed by the Etna Park authority (limiting the overall size and visual impact of the MEMS stations and making them non-permanent, fully removable infrastructures).
When deployed in the field, the MEMS station includes three main elements (Fig. 1): (i) the foldable steel structure holding the solar panel; (ii) the electronics case that contains the acquisition system, the router, the battery and the solar charge controller; (iii) the sensor box, hosting the gravity sensor. Besides robustness, another principle that drove the design of the field infrastructures for the MEMS devices is the use of low-cost, low-power and small-scale electronics components (IoT fashion). It is indeed the same challenge faced in the development of the MEMS gravimeters themselves: to produce low-cost and low-power devices, relying on integrated microsystems.

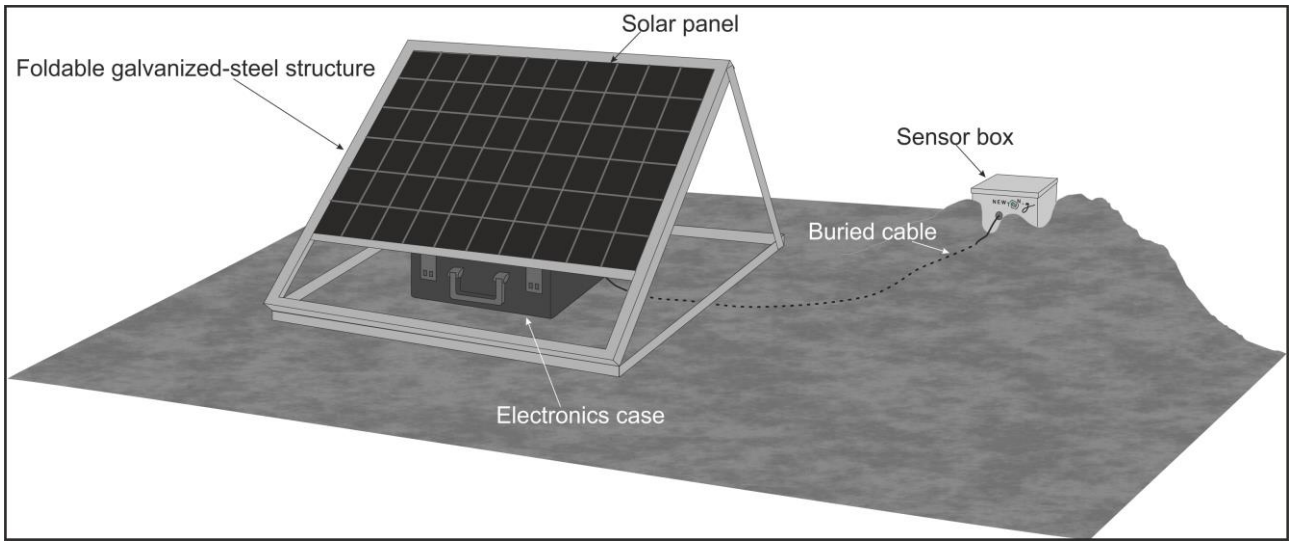

Figure 1 - Scheme showing the configuration of the typical MEMS station in the field. The main elements of the installation are: (i) the foldable steel structure holding the solar panel; (ii) the electronics case that contains the acquisition system, the router, the battery and the solar charge controller; (iii) the sensor box, hosting the gravity sensor.

2.1 Power supply system

Each MEMS station is powered through a photovoltaic panel, coupled with an Absorbed Glass Mat (AGM) lead-acid battery. To properly size this system, several issues were considered: the power required by the station (in terms of absorbed current, I_{abs}), the power supplied by the photovoltaic panel and the desired battery runtime without recharge (T_a). Table 1 reports the expected power consumption of a MEMS station.
Assuming a battery runtime of 72 hours, the usable capacity C_b of the battery should not be lower than:

$$C_{b\,min}\ (A_h) = I_{abs}\ (A) \times T_a\ (h) = 0.76 \times 72 = 54.7\ Ah$$

Device	Power (Wh)	I_{abs} (A) at 12V
MEMS gravimeter	5	0.42
Data logger	2	0.17
4G router	2	0.17
	Total: 9 Wh	**Total: 0.76 A**

Table 1 - Expected power consumption of a MEMS station

The recommended maximum depth of discharge (DoD) for AGM batteries is 50 to 75% of their nominal capacity; this limit should not be exceeded, to avoid damage to the battery and maximize its lifespan and performance. Considering $C_{b\ min}$, the nominal battery capacity should thus range between 75 Ah (DoD 75%) and 110 Ah (DoD 50%). The choice of the battery for the MEMS station was also constrained by its size and a suitable model was selected (see Table 2) with a nominal capacity of 90Ah and a size (especially in terms of height) fitting the electronic case.
The characteristics of the photovoltaic module must match the battery capacity and the expected solar radiation time. In winter time, when the useful solar radiation time (T_r) is approximately 7 hours, in order to ensure an efficient recharge of the 90Ah battery (maximum allowed DoD of 60%), the solar panel current I_p should be at least:

$$I_p = (C_{b\,60\%}(\text{Ah}) \times \mathit{eff}) / T_r(\text{h})) + I_{abs}\ (\text{A}) = 9.7\ \text{A}$$

eff is a coefficient related to the battery type, which, for AGM-type batteries, is 1.15. It is important to note that the above formula does not take into account the non-linear behaviour of lead-acid batteries during the last charging phase (between 80% and 100% of the capacity), which requires 4 hours to complete. This could imply a slightly longer full battery recharge time. The chosen photovoltaic panel for the MEMS stations (Table 2) offers a fair compromise between required $\mathbf{I_p}$ and physical size.

Component	Characteristics	Size (cm)	Model
Battery (AGM lead-acid)	12 V - 90 Ah	35x16.6x17.6	LUMINOR LGB12-90
Solar panel	200 W; peak curr.: 11.24 A	132x99x4	NX SOLAR - NX 200P
Solar charge controller	Type: MPPT Rated charge current: 15A Nominal PV pwr @ 12V: 220W	10x11x4	VICTRON ENERGY BlueSolar MPPT 75/15

Table 2 - Chosen components for the power supply system of a MEMS station

Three simulations were carried out, aimed to define the best tilt angle for the solar module. In particular, tilt angles of 30°, 50° and 60° were considered. Figure 2 shows the results of the simulations, in terms of (i) the total energy produced over a year and (ii) the monthly distribution of the produced energy. The 30° option allows the highest yearly energy (320 kWh/year), but with an uneven distribution of the energy produced throughout the year, i.e., important differences between summer and winter months (upper panel in Fig. 2). The 50° and 60° options (middle and lower panels in Fig. 2) provide similar patterns of yearly and monthly energy production. In both cases, the difference between energy produced in summer and winter is not as large as in the case of the 30° option. On the grounds of these results, the 50° option seems to be the best one, in terms of compromise between amount of power produced throughout a year and stability of the monthly production rate. Even though all the three considered options provide a much higher amount of power than required for the MEMS station (~80 kWh/year), long periods of reduced performance of the photovoltaic panel, due to, e.g., accumulation of snow and ice in winter, could still lead to interruptions in the functioning of the MEMS station.

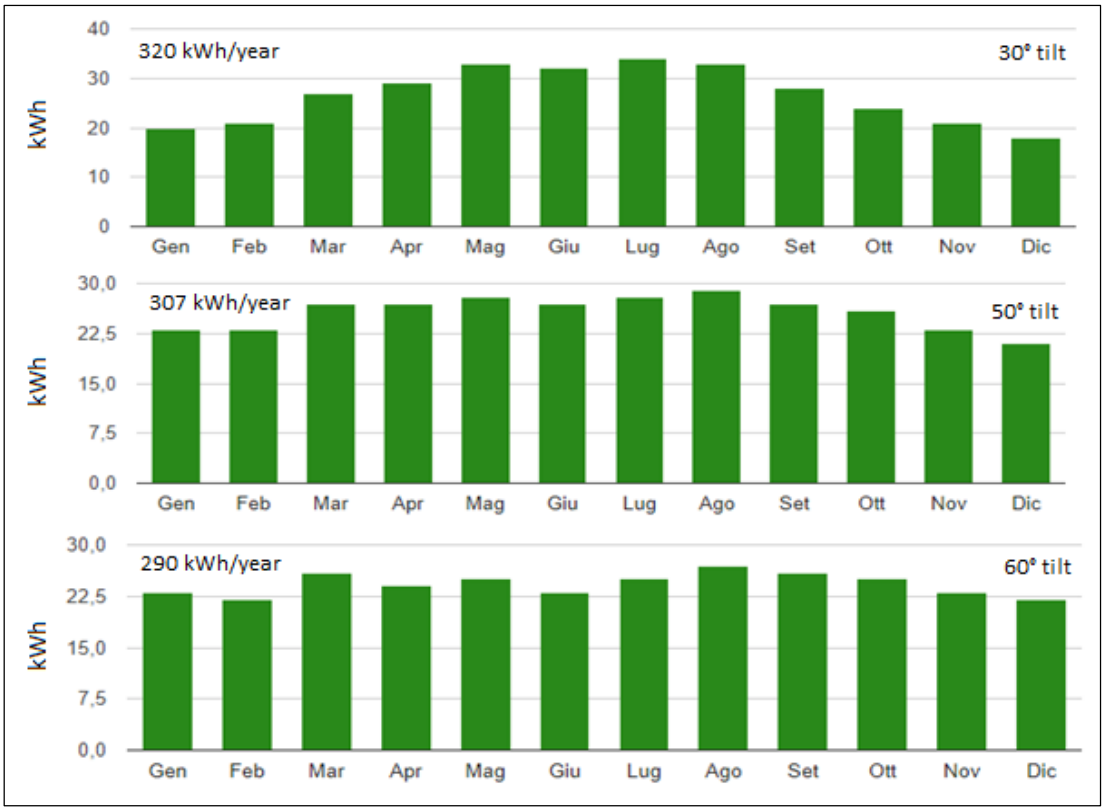

Figure 2. Yearly power supplied by a 200 W photovoltaic module on Etna. Three simulation were performed assuming different tilt angles of the photovoltaic module.

Figure 3 - Foldable galvanized-steel structure holding the solar panel of the MEMS station. The structure allows for different tilt angles of the panel.

At each MEMS station, the solar panel is mounted on a foldable galvanized-steel structure (Figs. 1 and 3), allowing to choose the tilt angle of the panel individually at each installation site, while also facilitating transport of the structure (and storage before installation). Its relatively heavy weight (about 70 kg) may pose a one-off challenge at locations where the installation site is not close to the road and must be reached on foot. Nevertheless, it makes the installation more able to withstand

strong winds.
The photovoltaic panel is connected to the battery through a solar charge controller (SCC); the latter handles the power produced by the photovoltaic module and uses it to properly and efficiently charge the battery. The most advanced SCCs on the market are based on the maximum power point tracking (MPPT) technology, which enables solar photovoltaic systems to harvest up to 30% more energy than conventional pulse width modulation (PWM) SCCs. Indeed, MPPT devices are capable of using the difference between output voltage of the panel and battery voltage to deliver more charging power, while with PWM systems this voltage difference is waisted.
The MEMS stations are equipped with a MPPT SCC (Table 2) which can handle a maximum photovoltaic open circuit voltage of 75 V and provide a maximum continuous load current of 15 A. This implies that all the power produced by the 200 W panel will be exploited, considering a charging voltage of 14 V and, thus, a current of 14.3 A (200 W / 14 V). The latter value is significantly higher than the minimum photovoltaic current (I_p = 9.7 A) required to recharge the station battery during winter time.

2.2 Data acquisition system

The electronics case (a compact IP67 plastic case; Fig. 1) contains all the devices that compose the data acquisition and transmission systems of the MEMS station (Fig. 4).
The data acquisition system was designed with the aim of making it as flexible, reliable and low-cost as possible.

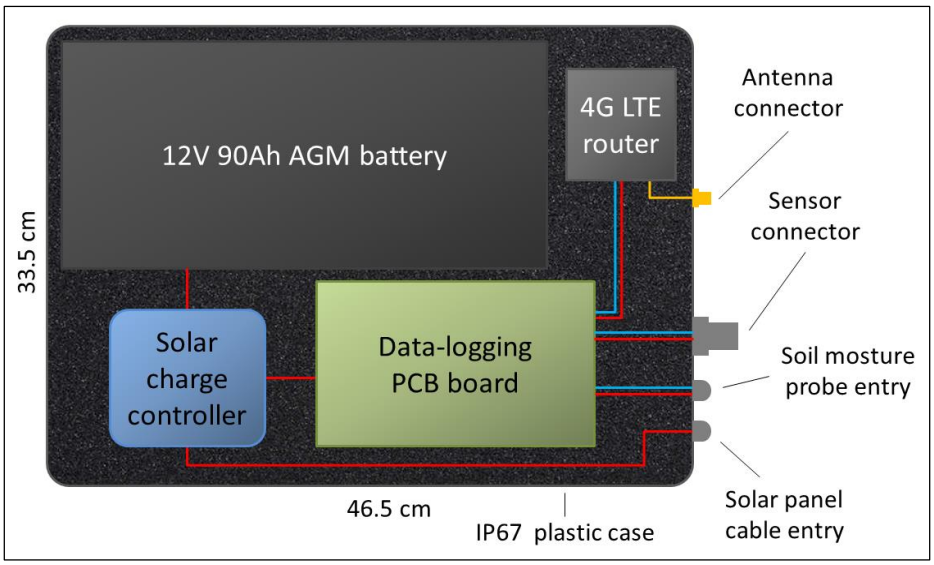

Figure 4 - Scheme showing the inside of the electronic case.

The main component of the data acquisition system is the Raspberry PI 3 model B+ (RPI), a low-power single-board computer. The RPI is mounted on a custom PCB board (called FASEL - NEWTON-g; Fig. 5), that also host a ATMega328PB (ATM) microcontroller and allows simple and reliable connection of the two devices to all the other components of the MEMS station. Both the RPI and the ATM feature very good computing performance, despite being low-cost and low-power consumer products. The RPI in the MEMS station runs the Raspbian Linux OS for ARM architectures. Through its General Purpose Input/Output (GPIO) interface, including up to 40 pins, the RPI can be connected to a very large variety of sensors. The MEMS gravimeter is connected through a Serial UART. Two BME280 sensors measuring air temperature, pressure and humidity are connected through I2C interface; one is integrated on the FASEL - NEWTON-g board (device n. 7 in Fig. 5), while the other is connected through a 4-pins terminal block (3.3V, GND, SCL, SDA).

Indeed, the second BME280 sensors is placed inside the sensor box (Fig. 1) to log environmental parameters that may affect the output from the gravimeter. The MEMS station can also be equipped with one or more Truebner SMT100 soil moisture probes, able to measure the water content, permittivity and temperature of the terrain. Indeed, a dedicated terminal block on the PCB board (n. 4 in Fig. 5) allows direct connection of the probe(s). The Truebner SMT100 is a SDI-12 device, thus only 3 pins are needed, two for 5V powering, the other one for asynchronous serial data communication. The ATM queries the probe(s), retrieve the data and redirect them to the RPI, through I2C protocol. More than one probe can be connected to the PCB board, using a suitable water-proof split box.

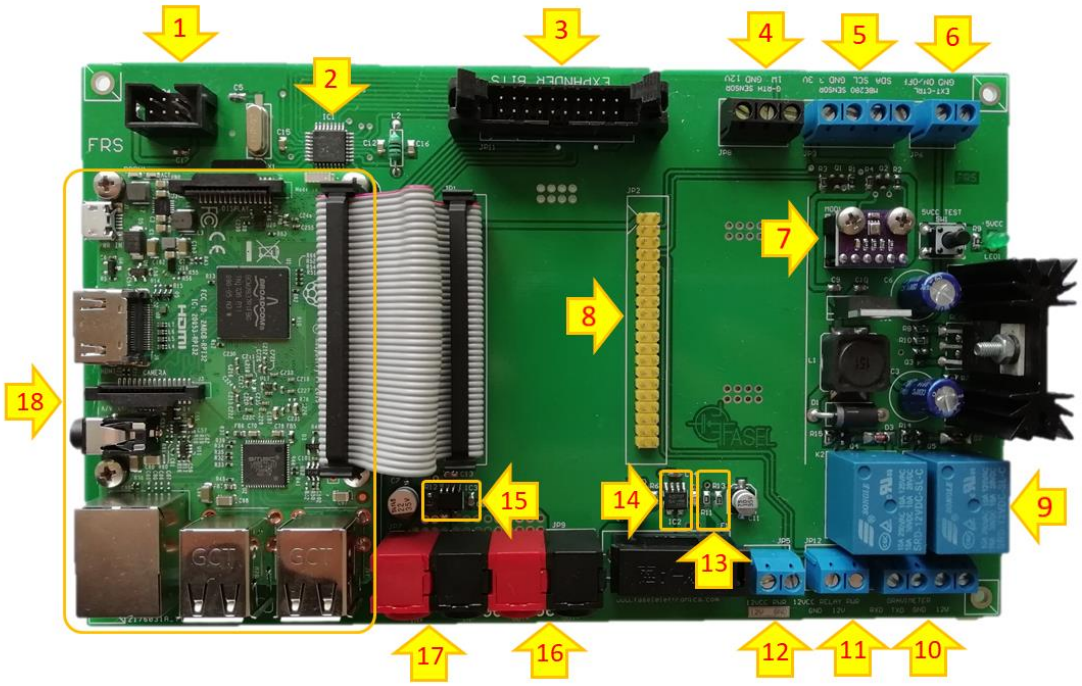

Callout	Description	Callout	Description
1	ISP connector for ATmega programming	10	Gravimeter connector (data and power)
2	Atmel ATmega328PB microcontroller	11	RUT240 router connector (only power)
3	Atmega I/O expansion bits	12	Main 12V DC IN power supply
4	Soil mosture probe connector	13	Voltage divider for battery volt. measure
5	External BME280 sensor connector	14	ACS712T-ELC-05B for load current measure
6	Incoming open collector from RUT240	15	ACS712T-ELC-20A for PV current measure
7	On-board BME280 sensor	16	Photovoltaic panel OUT connectors
8	Raspberry PI 3 GPIO lines	17	Photovoltaic panel IN connectors
9	2 x Relays connected to 10 and 11	18	Raspberry PI 3 model B+ board

Figure 5 - The FASEL - NEWTON-g PCB board

The FASEL - NEWTON-g board is also equipped with a voltage divider for battery monitoring and two ACS712 current sensors (n. 13, 14 and 15 in Fig. 5). They are managed by the ATM, through its analog input lines (10 bits ADC), and allow to measure (i) the battery voltage, (ii) the current provided by the photovoltaic panel (produced) and (iii) the current flowing to the devices (consumed). Through these parameters the state of health (SOH) of the MEMS station is tracked.
Custom software was developed to perform real-time data acquisition. The main data-logging software, running on the RPI, was written in Python, while the ATM was programmed in Wiring

language, through the Arduino IDE. Data from the MEMS device (gravity and complementary parameters) are acquired at a rate of 1 sample/sec, through a program which is launched at system boot and is always running. In the framework of a master-slave protocol, the RPI (master) performs sequenced requests to the MEMS sensor (slave), which responds by supplying the current set of values. System SOH and environmental parameters are logged through another Python code that is launched once a minute. During its execution, the RPI performs a I2C data request to ATM, which provides the latest voltage/current and soil moisture set of values.
Data are stored locally, in the on-board 64GB microSD memory of the RPI. They are organized in three different categories of ASCII files. Table 3 reports all the parameters that are acquired by a MEMS station.

Samp. Freq.	Category	Description	Code	Sensor
1 sp/sec	Gravimeter	Gravity Value	GRAV.VAL	MEMS Gravimeter
	Gravimeter	MEMS (core) Temperature	GRAV.TMP1	MEMS Gravimeter
	Gravimeter	Enclosure Temperature	GRAV.TMP2	MEMS Gravimeter
	Gravimeter	Tilt X Level	GRAV.XLEV	MEMS Gravimeter
	Gravimeter	Tilt Y Level	GRAV.YLEV	MEMS Gravimeter
	Gravimeter	MEMS Pressure	GRAV.BARO	MEMS Gravimeter
	Gravimeter	MEMS Humidity	GRAV.HUM	MEMS Gravimeter
1 sp/min	Environmental	Sensor Box Temperature	BOX.TEMP	External BME280
	Environmental	Sensor Box Pressure	BOX.BARO	External BME280
	Environmental	Sensor Box Humidity	BOX.HUM	External BME280
	Environmental	Soil Permittivity	SOIL.PERM	SMT100 Probe
	Environmental	Soil Water Content	SOIL.WTC	SMT100 Probe
	Environmental	Soil Temperature	SOIL.TEMP	SMT100 Probe
1 sp/min	System SOH	Battery Voltage	BATT.VOLT	Voltage Divider
	System SOH	Current on Load	LOAD.CURR	ACS712
	System SOH	Current from Solar Panel	PTVC.CURR	ACS712
	System SOH	RPI CPU Temperature	CPU.TEMP	Raspberry PI
	System SOH	Electronics Case Temperature	CASE.TEMP	On-board BME280
	System SOH	Electronics Case Pressure	CASE.BARO	On-board BME280
	System SOH	Electronics Case Humidity	CASE.HUM	On-board BME280

Table 3 – List of the parameters that are acquired at each MEMS station

Data collected at a rate of 1 sp/sec are stored in daily files, while data collected at 1 sp/min rate are stored in monthly files.

2.3 Data transmission system

Data collected and stored locally by each MEMS station in the gravity imager must be regularly transferred to the central acquisition server, at INGV-OE, in Catania, which acts as “data concentrator” (Fig. 6). For data transmission from the remote installation sites, cellular network technology was preferred over other possible options, such as 5 GHz Wi-Fi or UHF band serial transmission. Even though the latter are both widely used technologies for remote transmissions, they suffer significant drawbacks. UHF systems are low-power and they usually perform properly even over long distances, even though problems of radio visibility often occur. The most impotant drawback is the lack of LAN connectivity (UHF devices handle serial transmission only), implying that they preclude the use of protocols based on the TCP(UDP)/IP suite, such as FTP, SSH and VNC. Wi-Fi systems allow LAN connectivity, but they are power-hungry and do not transmit over

long distances. A transmission infrastructure of point-to-point links must thus be built to reach a site where Internet access is available (gateway). Conversely, the 4G LTE technology provides a direct Internet access, ensuring a suitable bandwidth for remote interactivity from/to the data-logging devices of the MEMS stations. Several surveys were performed in the target installation area (summit of Mt Etna), and good 4G coverage was found at most sites. MEMS stations are thus equipped with a 4G/LTE router (Teltonika RUT240), which is able to connect to a mobile operator infrastructure and share the internet connection through its Ethernet interface.
The synchronization strategy between MEMS stations in the field and the central data concentrator in Catania is based on Rsync, a Linux-based remote and local file synchronization tool. It is faster than other tools because it implements a differential backup protocol, meaning that only differences between the two datasets are transferred. Furthermore, Rsync requires less bandwidth as it performs data compression and decompression during data transmission. In the framework of NEWTON-g, the “over SSH” version of Rsync is used, allowing the encryption of the connection.
Data transmission tests have already been performed from a prototype MEMS station, installed in the summer of 2019 (southern slope of the volcano, at an elevation of about 2300m; see Deliverable 3.2). The data synchronization (scheduled to be executed every 3 hours) has worked properly, thus proving the reliability of the chosen tools.
Data produced by the MEMS stations will be stored on the INGV-OE concentrator server, which will be accessible to all NEWTON-g partners through conventional protocols for data sharing over the Internet, such as FTP (Fig. 6).

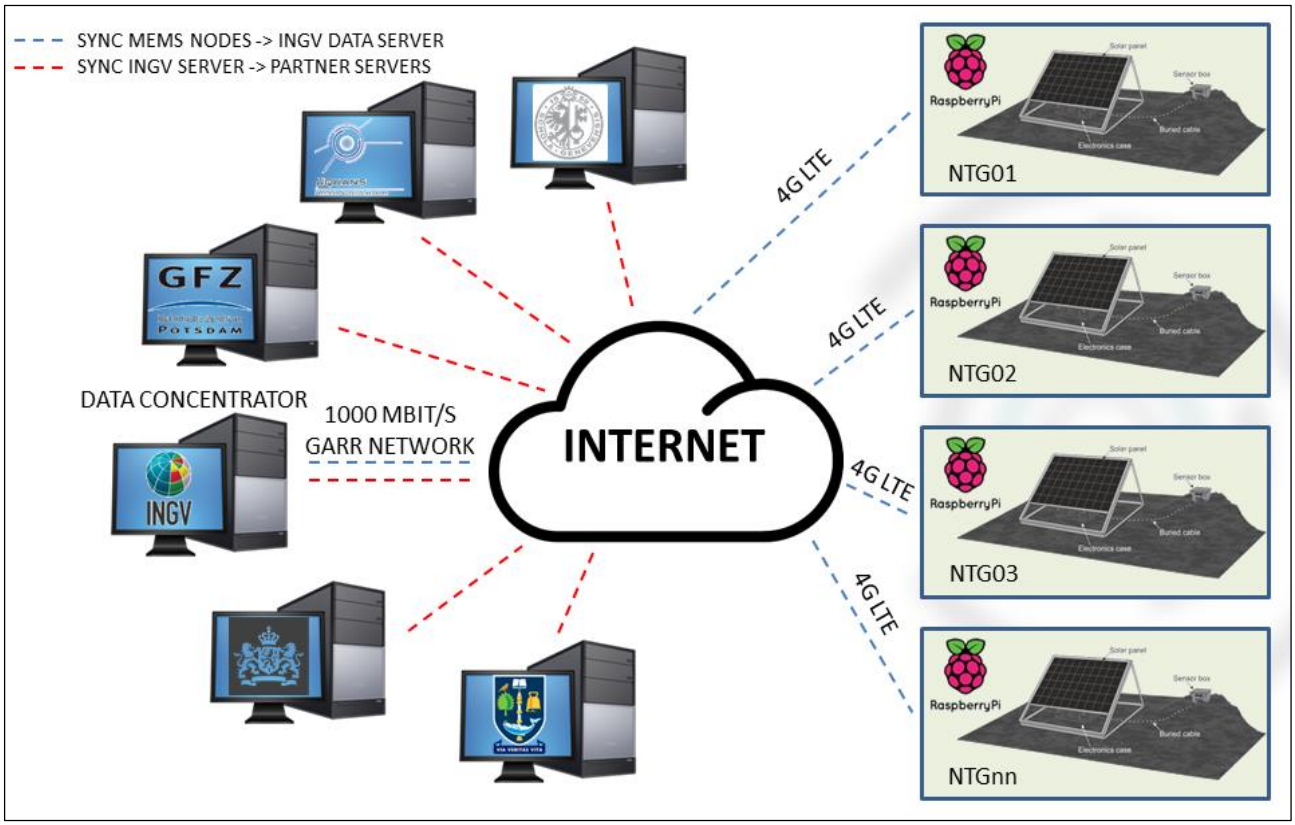

Figure 6 - Scheme showing the architecture of NEWTON-g data transmission and sharing.

2.4 Sensor box

An IP67 PVC box (sensor box in Fig. 1) is used to protect the MEMS sensor from external perturbations. At each installation site, a thin layer of self-leveling concrete is poured, aimed to ensure suitable coupling of the sensor to the base rock (Figs. 7 and 8). The sensor box is anchored

on the flat and level concrete base. The bottom of the sensor box is partly removed to decouple it from the gravimeter (Figs. 7 and 8). The latter is placed directly on the concrete in order to avoid transmission of shocks and vibrations of the external housing. Watertight, heavy-duty connectors and cable are used to route power and signals between sensor box and electronics case.
The reliability of this design was checked in the framework of field tests performed during the summer of 2019 (see Deliverable 3.2).

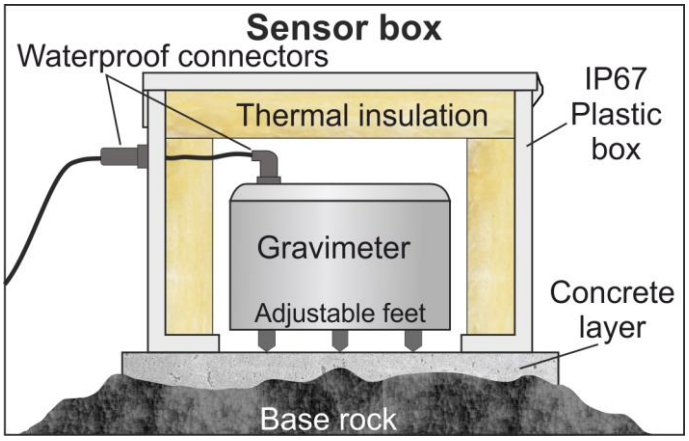

Figure 7 – Sketch cross-section across the sensor box installed in the field. The box is anchored to the concrete layer which ensures a suitable coupling of the MEMS sensor to the base rock. The bottom of the sensor box is partly removed to decouple it from the gravimeter.

Figure 8 – Left: concrete base on Etna at 2900m elevation. The summit active craters are visible in the background. Right: bottomless PVC box, installed on Etna at 2600m elevation, in the framework of field-tests during the summer of 2019 (see Deliverable 3.2 for details). In the final setup, a PVC box different from the one shown here is utilized.

3. Off-grid power system for the AQG-B at Pizzi Deneri

3.1 Installation site of the AQG-B on Etna

As reported in D2.1, the first choice for the installation site of the AQG-B on Etna is the Volcanological Observatory of Pizzi Deneri (northern slope of Etna; 2800 m elevation; Fig. 9). The only viable alternative is the Astrophysical Observatory of Serra La Nave (SLN; southern slope of the volcano; 1730 m elevation; Fig. 9). At Serra La Nave mains electricity is available and the installation of the AQG-B would not pose significant challenges. Nevertheless, this site is relatively far from the active summit craters of Etna (about 6.5km; Fig. 9), hence only minor gravity changes are expected to develop in response to most volcanic processes. Furthermore, a superconducting gravimeter has acquired continuous data at this site since 2014 (iGrav#16; Carbone et al., 2019), implying that having the quantum gravimeter operating at this site would provide partially redundant information.
PDN is much closer to the summit of Etna (~2.7 km from the summit carters; Fig. 9) than SLN and measurable gravity changes are expected to occur at this site, due to volcano-driven mass redistribution in the shallow plumbing system of Etna (Carbone et al., 2015). Continuous gravity measurements were accomplished at PDN using spring gravimeters and provided important results (Carbone et al., 2003), thus proving the strategic position of this site from the point of view of volcano monitoring through gravimetry. Currently, no continuous gravity observations are carried out at PDN and the installation of the quantum gravimeter at this site would thus provide unique and valuable data. Accordingly, PDN is the target installation site for the AQG on Etna. It is important to also note that in the basement of the PDN Volcanological Observatory there is a stable concrete pillar, detached from the rest of the building, which has been used, since 2007, for the execution of periodic absolute gravity measurements. Furthermore, an already existing Wi-Fi link allows data transfer from PDN to the headquarters of INGV-OE.

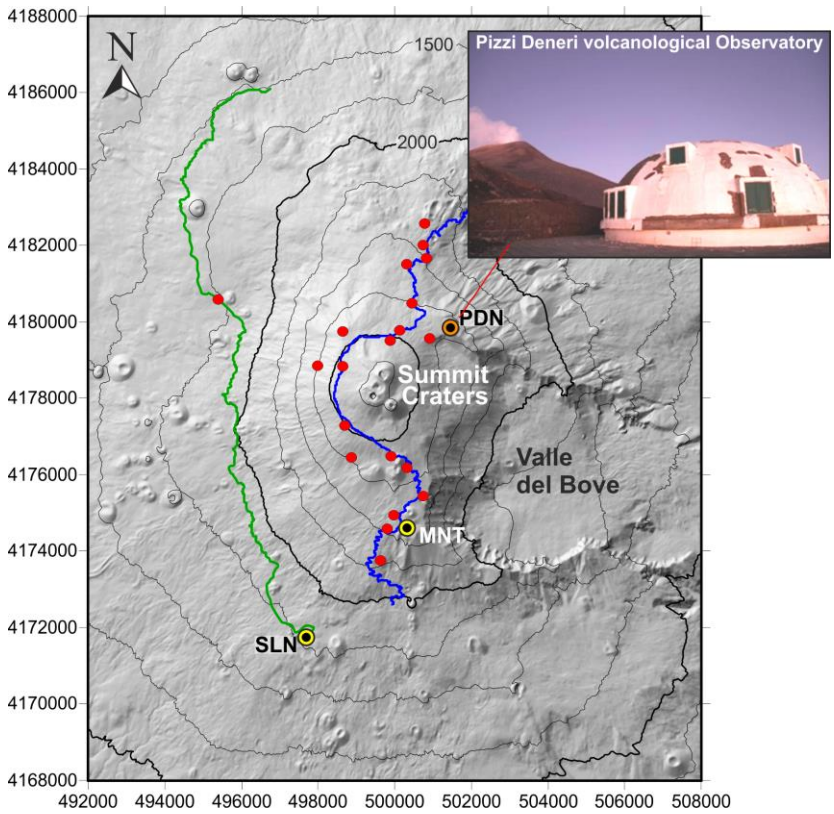

Figure 9 – Sketch map of Mt. Etna showing the position of the Pizzi Deneri Volcanological Observatory (PDN) and the two uppermost continuous gravity stations of the INGV-OE monitoring system (SLN and MNT). The red dots indicate the most likely configuration of MEMS stations. The blue and green tracks mark the Summit and Forestale roads. The inset on the top right shows a photo of the PDN observatory.

3.2 Design of the off-grid power system

The AQG-B runs on 220V AC and requires around 500 W of continuous power. Mains electricity is not available at PDN, implying that an off-grid power supply system must be installed to allow continuous gravity measurements through the AQG-B. Different off-grid power sources have been considered to fulfill the power requirements of the gravimeter, including solar panels, fuel cells, diesel generators and wind generators. Solar panels are only effective during daily hours of bright sunshine and may be ineffective due to clouds and ash cover. In winter, snow may completely cover the panel surface. Because solar power is unreliable on its own, it is not a good candidate for sole use, especially considering that the quantum gravimeter should work continuously. However, solar power can contribute to other power installations. Wind speed on Mt. Etna can be extreme and a wind turbine is not considered a good candidate as it could easily get damaged. A hybrid solution with solar panels and methanol fuel cells would have a too high total cost and would be difficult to maintain, since about six methanol 60-liter tanks would be needed to power the gravimeter for roughly 30 days (see also Deliverable 3.2).

The most reliable and affordable off-grid solution to power the AQG-B at PDN is a hybrid system, including solar panels and a diesel generator, as the power sources. This system also comprises a large stack of batteries to store the power generated by the two sources. Besides power sources and accumulators, the hybrid off-grid system is equipped with a photovoltaic inverter and a battery management system (BMS). The photovoltaic inverter handles the current produced by the solar panels, converts DC to AC and makes the flow available to the BMS. The latter works as a grid manager that (i) regulates the balance between energy fed to the grid and energy used by the load and (ii) ensures proper storage of the energy in the accumulators, to guarantee a continuous power supply. The reliability and efficiency of the BMS is based on precise determination of the state of charge. Overcharging and deep discharging of the accumulators are safely avoided, thus enabling an optimum exploitation of the battery capacity.

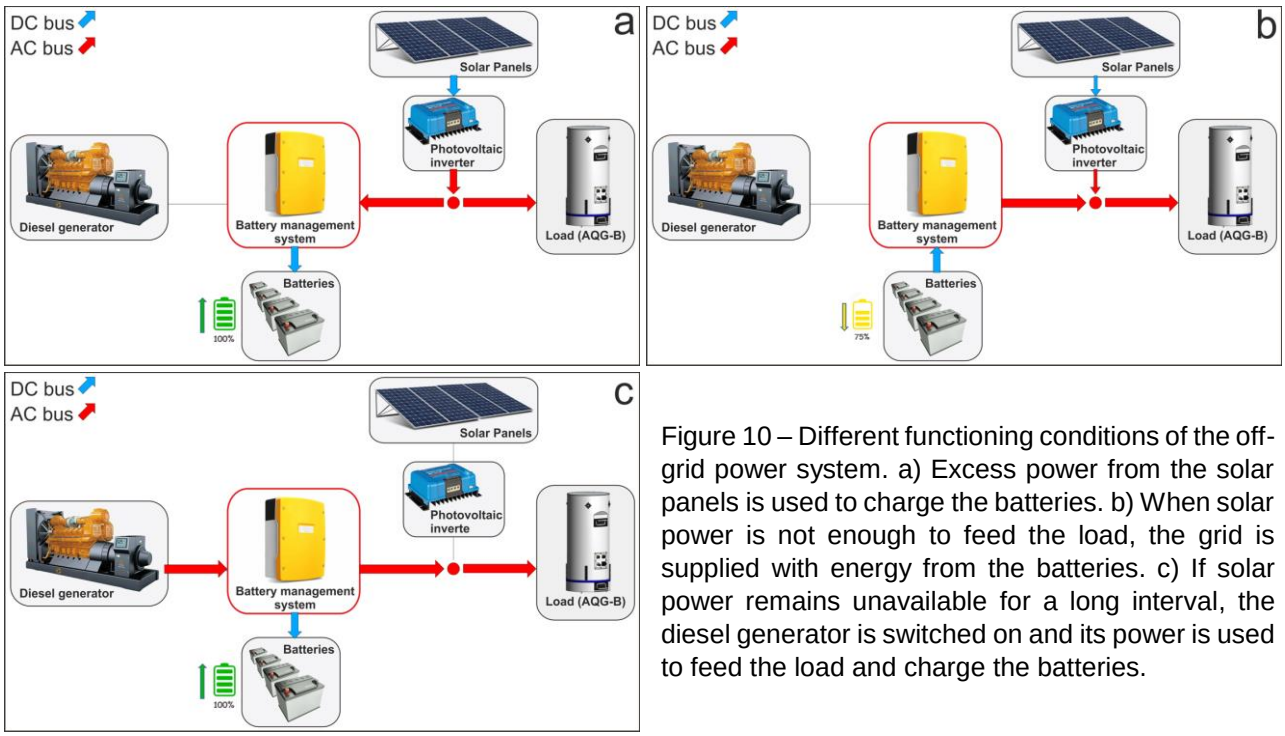

Figure 10 – Different functioning conditions of the off-grid power system. a) Excess power from the solar panels is used to charge the batteries. b) When solar power is not enough to feed the load, the grid is supplied with energy from the batteries. c) If solar power remains unavailable for a long interval, the diesel generator is switched on and its power is used to feed the load and charge the batteries.

The powering/charging source is automatically switched between solar panels and diesel generator, depending on the solar power available at a certain time. If the available solar power exceeds the power demand from the load, the BMS redirect the excess power to charge the batteries (Fig. 10a). Conversely, if the available solar power is not enough to supply the load, the BMS automatically

compensates the power gap through supplying the grid with energy from the batteries (Fig. 10b). If solar power remains unavailable for a long interval and the battery level drops below a certain threshold, the BMS switches the diesel generator on and uses its power to supply the load and charge the batteries (Fig. 10c).
The dimensioning of the various components of the hybrid system depends on the trade-off between the following factors: (i) the need to minimize the average working time of the diesel generator, in order to reduce diesel consumption; (ii) the available surface area for solar panels in the facilities of the PDN observatory, which constraints the number of modules one can install; (iii) the need to supply continuous and uninterrupted power supply to the quantum gravimeter.
The specifications of the chosen components for the off-grid system to be installed at PDN are indicated in Table 4.

Component	Characteristics	Size (cm)	Model
Battery pack (lithium-ion)	Capacity: 156.6 Ah Energy content: 8.5 kWh	64x42x49	BMZ Energy Storage System ESS 9.0
Solar panels (10 modules)	Peak power: 350 W 10.27 A @ 34.07 V	174x103x3	QCELLS - QPEAK DUO 350
Photovoltaic inverter	Nominal Power (@ 230 V): 3 kW Max output current: 16 A	43x47x18	SMA Sunny Boy 3.0-1AV-41
Battery management system (with inverter)	Max AC power: 3.3 kW Max AC current: 14.5 A	47x61x24	SMA Sunny Island 4.4M-13
Diesel generator	Max power (@ 230 V): 5.4 kW Continuous power: 4.4 kW	99x60x83	Pramac P6000

Table 4 - Chosen components for the off-grid power system for the AQG-B at PDN.

3.3 Expected performances

Functioning characteristics of the off-grid power system are reported in Table 5.

POWER	
Total number of PV modules	10
Peak power	3.50 kWp
Nominal AC power of the PV inverters	3.00 kW
AC active power	3.00 kW
ENERGY (yearly)	
Annual energy consumption	4400 kWh
Annual max. available PV energy	5694 kWh
Used PV energy (annual)	3390 kWh
Directly consumed PV energy	1712 kWh
Intermediately stored PV energy	1678 kWh
Annual energy from the diesel generator	1832 kWh
Annual fuel consumption	625 l

Table 5 – Expected performance of the off-grid power system for the AQG-B at PDN.

4. Impact of the COVID-19 pandemic

The lockdown imposed by the Italian government to fight the spread of the COVID-19 pandemic, with effect from mid-March 2020, has affected the ability of the INGV-OE team to respect the timetable agreed during the pre-deployment meeting (Catania, 5-7 February 2020).
In February 2020 the design of both (i) MEMS station and (ii) off-grid power system for the AQG-B at PDN was complete and five administrative procedures were started, aimed to purchase all the needed materials and services.
The enforced shut down has impacted the course of the above procedures, mainly due to the difficulties encountered by the administrative staff of INGV-OE in handling some steps of the procedures, while working from home during social isolation. As a consequence, the administrative procedures have taken 1 to 3 months longer to complete than originally planned. At the time of this writing (end of May 2020), 4 out of the 5 procedures are completed, while only the last formal steps are needed to complete the 5th procedure. The INGV-OE team is in contact with the companies in charge of providing the needed materials and services. Unfortunately, further delays could arise due to suppliers having some items out-of-stock, as a consequence of the COVID-19 crisis.

4.1 Impact on the installation of the off-grid power system at PDN

During the pre-deployment meeting, the consortium agreed that the installation of the off-grid system to power the AQG-B at PDN should occur between 21 June and 3 July 2020. This installation comprises different activities: building the external structure to hold the solar panels in place, wiring the external (solar panels) and internal components of the off-grid system, ensuring that all the devices are properly and safely installed and connected, setting the grid-relevant parameters in the BMS and PV inverter. Three different companies are in charge of supplying materials and services to complete the installation.
Under the best-case scenario, assuming that the purchased goods will be delivered within 5 weeks after receipt of the orders, it should be possible to perform the installation of the off-grid power system at PDN sometimes between the 2nd and 4th week of July 2020. This would allow to respect the agreed schedule for the installation of the AQG-B at PDN (between the last week of July and the 1st week of August 2020). Indeed, as reported in D2.4 (Quantum device prototype), MUQUANS estimates that, despite the impact of the COVID-19, it is still feasible that the AQG-B will be shipped to Sicily within the agreed timeline, i.e., between the 4th and 5th week of July 2020.
Under the worst-case scenario, if the delivery of the orders takes much longer than 4 – 5 weeks, it will be necessary to postpone the installation of the off-grid system either to a later time during the summer of 2020, or to the spring/summer of 2021, if all the needed materials are not available before PDN becomes unreachable by car because of the snow cover.

4.2 Impact on the assembling and installation of the MEMS station

During the pre-deployment meeting, the consortium agreed to install the first 10 MEMS stations (equipped with gravimeters) within the 3rd week of July. The installation of the MEMS stations was scheduled to start in late May and continue throughout June and July 2020.
The COVID-19 pandemic affected the administrative procedure to purchase the needed items for assembling the MEMS stations. Indeed, the purchase order was issued on 27 May, ~2 months later than planned. Assuming a delivery time of 4 – 5 weeks, the INGV team should have the needed materials at its disposal by the end of June/beginning of July 2020.
As reported in D2.5 (MEMS device prototype), the COVID-19 pandemic has severely impacted the NEWTON-g-related activities of the UNIGLA-IGR team, due to the shutdown of university facilities, like the JWNC and the Kelvin Building, that are required for any R&D and fabrication of the MEMS gravimeters. Under the best-case scenario, the UNIGLA-IGR team foresees that no more than 1-2 MEMS gravimeters will be available for installation on Etna by the end of autumn 2020.
Regardless, during July and August 2020 the INGV-team will install some MEMS stations (without the gravimeters) at different elevations on Etna, in order to field-test the performance of the different

systems described in section 2. The stations will be fitted with the MEMS gravimeters once they become available.

REFERENCES

Carbone, D., Budetta, G., Greco, F. & Rymer, H., 2003. Combined discrete and continuous gravity observations at Mount Etna. J. Volcanol. Geotherm. Res., 123 (1–2), 123–135. doi: 10.1016/S0377-0273(03)00032-5.

Carbone, D., Zuccarello, L., Messina, A., Scollo, S. and Rymer, H., 2015. Balancing bulk gas accumulation and gas output before and during lava fountaining episodes at Mt. Etna. Sci. Rep. 5, 18049, doi:10.1038/srep18049.